

Towards a Resolution of the Galactic Spin Crisis: Mergers, Feedback, and Spin Segregation

Ariyeh H. Maller and Avishai Dekel

Racah Institute for Physics, The Hebrew University, Jerusalem 91904, Israel

1 February 2008

ABSTRACT

We model in simple terms the angular-momentum problems of galaxy formation in CDM cosmologies, and identify the key elements of a scenario that may solve them. The buildup of angular momentum is modeled via dynamical friction and tidal stripping in a sequence of mergers. We demonstrate how over-cooling in incoming halos leads to a transfer of angular momentum from the baryons to the dark matter, in conflict with observations. By incorporating a simple recipe of supernova feedback, we are able to solve the problems of angular momentum in disk formation. Gas removal from the numerous small incoming halos, which merge to become the low specific angular momentum (j) component of the product, eliminates the low- j baryons. Heating and puffing-up of the gas in larger incoming halos, combined with efficient tidal stripping, reduces the angular momentum loss of baryons due to dynamical friction. Dependence of the feedback effects on the progenitor halo mass implies that the spin of baryons is typically higher for lower mass halos. The observed low baryonic fraction in dwarf galaxies is used to calibrate the characteristic velocity associated with supernova feedback, yielding $V_{fb} \sim 100 \text{ km s}^{-1}$, within the range of theoretical expectations. We then find that the model naturally produces the observed distribution of the spin parameter among dwarf and bright disk galaxies, as well as the j profile inside these galaxies. This suggests that the model indeed captures the main features of a full scenario for resolving the spin crisis.

Key words: cosmology – dark matter – galaxies:formation – galaxies:spiral

1 INTRODUCTION

The ‘standard’ model of cosmology, which assumes hierarchical buildup of structure in a universe where the mass is dominated by cold dark matter (CDM), seems to be facing intriguing difficulties in explaining some of the robust observed properties of galaxies. Standing out among these problems is the inability of galaxy formation models to reproduce both the sizes and structure of disk galaxies. In hydrodynamical simulations baryons lose a significant fraction of their angular momentum leading to overly small disks. To avoid this, analytic and semi-analytic models commonly assume there is no angular momentum loss. Recent studies, however, show that this leads to a variety of discrepancies with observations. Taken together this suggests a crisis in our understanding of the role of angular momentum in forming disk galaxies. Our aim here is to make progress in the effort to resolve this crisis by first reproducing the problems using a simple model in which the important physical ingredients are spelled out and well understood. Subsequently we incorporate an additional process into this model which

then reproduces the observed sizes and structure of galactic disks.

The sizes of galactic disks are commonly linked to the angular momentum of their parent dark-matter halos (Fall & Efstathiou 1980). This modeling is based on the distribution of halo spin parameters as found in N-body simulations (see Bullock et al. 2001, and references therein), combined with the assumptions that the baryons and dark matter initially share the same distribution of specific angular momentum, j , within the halos (as seen in simulations by van den Bosch et al. 2002) and that j is conserved as the baryons contract to form the disk (as suggested by Mestel 1963). The sizes of disks obtained under these assumptions are roughly comparable to those observed.

However, high-resolution simulations that incorporate gas processes find this scenario to be invalid. In particular, they find that a significant fraction of the angular momentum of the baryons is transferred to the dark matter, resulting in disk sizes roughly an order of magnitude smaller than those observed (Navarro & Steinmetz 2000; Sommer-Larsen et al. 1999; Navarro & Steinmetz 1997; Navarro et al. 1995;

Navarro & Benz 1991). This has been referred to as the *angular momentum catastrophe*.

The angular momentum catastrophe is commonly associated with the problem of “over-cooling” in CDM-type scenarios (White & Frenk 1991; White & Rees 1978). Without sufficient feedback much of the gas cools quickly, contracts into small halos and then spirals deep into the centers of bigger halos, efficiently transferring its orbital angular momentum to the dark matter (Navarro & Steinmetz 2000). It has therefore been speculated that enough energy feedback from supernova may prevent this over-cooling (Larson 1974; White & Rees 1978) and thus reduce the angular-momentum loss. Indeed, simulations where gas cooling is artificially suppressed till $z = 1$ do not suffer from the angular momentum catastrophe (Eke et al. 2000; Weil et al. 1998). Furthermore, simulations including some forms of feedback show a reduction in the amount of angular momentum lost (Sommer-Larsen et al. 1999). However, while feedback has been studied using simplified approximations (e.g., Dekel & Silk 1986, hereafter DS), a realistic implementation of feedback has proved challenging (see Thacker & Couchman 2000, and references therein), though some partial progress may have been made recently (Ferrara & Tolstoy 2000; Thacker & Couchman 2001; Springel & Hernquist 2002). At this point, the feedback scenario has not yet been studied in satisfactory detail, nor has it been confirmed to solve the spin problem, or properly understood in basic terms. This motivates an attempt to understand the scenario and how it may work using a simple semi-analytic model, in which the basic elements are easily understood.

Even if the angular momentum catastrophe can be avoided such that the total baryonic spin agrees with the total dark-halo spin, there remain discrepancies between the angular-momentum properties of dark halos in N-body simulations and those of observed disk galaxies. Foremost among these is the apparent mismatch of the distribution of specific angular momentum within galaxies (loosely termed “the j profile”) between observations and N-body simulations. Bullock et al. (2001, hereafter BD) revealed a universal profile with an excess of both low- j and high- j material compared to the observed j distribution in exponential galactic disks. Subsequently, van den Bosch, Burkert & Swaters (2001, hereafter BBS) have measured the j distribution in a sample of dwarf disk galaxies, confirming in detail, case by case, the differences between the j profile predicted by the simulated halos and those found in disk galaxies. We refer to this second discrepancy as the *mismatch of angular-momentum profiles*.

Another spin problem is indicated by the observations of de Jong & Lacey (2000), who found that the scatter in the log of the spin parameter inferred from fitting the spread of observed disks sizes in a large sample of late-type disk galaxies is only 0.36 ± 0.03 , while the scatter seen in simulated halos is significantly larger, 0.5 ± 0.05 (BD and references therein). This could have been explained by a scenario in which the disks formed in low-spin halos are unstable and thus become early-type galaxies, which implies that disk galaxies occupy only the higher spin halos (Mo, Mao & White 1998; van den Bosch 1998). However, this scenario is in apparent conflict with the finding in N-body simulations that recent major mergers, usually identified with large spheroidal components, actually give rise to halos with

higher spin than average (Gardner 2001; Wechsler 2001). This demonstrates that the exact connection between the angular-momentum properties observed in galaxies and in N-body simulations is unclear.

We propose that the solution to the crisis is spin segregation — that the angular momentum distribution of baryons differs from that of the dark matter due to gas processes. These processes can either decrease or increase the specific angular momentum of the baryons relative to the dark matter. Gas cooling generally results in lower spin for the baryons compared to the dark matter, but heating due to feedback reduces this effect, and gas removal in small halos actually results in a higher spin for the baryons compared to the dark matter.

In this paper we work out a simple model to explore these effects. Knowing that in a hierarchical scenario the halo buildup can be largely interpreted as a sequence of mergers between smaller halos, our model is based on a simple algorithm for the buildup of halo spin by summation of the orbital angular momenta of merging satellites (Maller et al. 2002; Vitvitska et al. 2001). This algorithm has been found to match well the spin distribution among halos in N-body simulations. In this paper we extend the model and find that it also reproduces the angular-momentum profile within halos. It therefore provides a useful insight into the origin of the spin problems, and a clue for their possible solution. We therefore use this model as a tool for incorporating the relevant baryonic processes, and especially feedback.

In §2 we describe the model for angular-momentum buildup in halos by mergers. In §3 we model the angular momentum catastrophe as resulting from over-cooling and dynamical friction. In §4 we introduce a simple model of feedback. In §5 we study the resultant angular-momentum properties of the baryonic component both in bright and dwarf disk galaxies and compare them to observations. In §6 we test the robustness of our results to the details of the feedback model assumed. We conclude and discuss our results in §7.

2 BUILDUP OF HALO SPIN BY MERGERS

2.1 Modeling the Spin Parameter

The angular momentum of a galaxy, J , is commonly expressed in terms of the dimensionless spin parameter $\lambda = J\sqrt{|E|}/GM^{5/2}$, where E is the internal energy (Peebles 1969). In practice, the computation and measurement of this quantity, especially the energy, may be ambiguous, e.g., it is not obvious how to define separate spin parameters for the dark matter and the baryons. Furthermore, it introduces an undesired dependence on the specifics of the halo density profile. Instead, following BD, we use the modified spin parameter

$$\lambda' = \frac{j}{\sqrt{2}V_{\text{vir}}R_{\text{vir}}}, \quad (1)$$

where $j = J/M$ is the specific angular momentum. This quantity is more straightforward to compute for each component, λ'_{dm} and λ'_b , and it does not explicitly depend on the density profile of the halo. For a density profile of the type suggested by Navarro et al. (1996, NFW) λ' is related

to λ by

$$\lambda' = \lambda f_c^{-1/2}, \quad (2)$$

where the factor f_c reflects the difference between the energy of an NFW halo and a truncated singular isothermal sphere. An expression for f_c as a function of the halo concentration, c_{vir} , is given in Mo et al. (1998, equation 22). For a NFW halo with $c_{\text{vir}} = 4.5$ the values of the two spin parameters become equal.

BD found for simulated halos that, similarly to λ , the distribution of λ' is well fit by a log-normal function,

$$P(\lambda') d\lambda' = \frac{1}{\sqrt{2\pi\sigma_\lambda^2}} \exp\left(-\frac{\ln^2(\lambda'/\lambda'_0)}{2\sigma_\lambda^2}\right) \frac{d\lambda'}{\lambda'}, \quad (3)$$

with $\lambda'_0 \simeq 0.035$ (compared to $\lambda_0 \simeq 0.042$) and $\sigma_\lambda \simeq 0.5$.

In Maller et al. (2002), we proposed a very simple model for the buildup of spin in dark halos, termed “the orbital-merger model”. In this model, the spin of a final halo is simply the vector sum of the orbital angular momenta of all the halos merging into its main progenitor throughout its history. In this paper, as in Maller et al. (2002), we generate 500 random realizations of merger histories for each desired final halo mass at $z = 0$, using the method of Somerville & Kolatt (1999) with the slight adjustment of Bullock, Kravtsov & Weinberg (2000) to implement the Extended Press Schechter formalism (Lacey & Cole 1993; Bond et al. 1991). The specific cosmology assumed, without significant loss of generality, is the “standard” Λ CDM cosmology, with $\Omega_m = 0.3$, $\Omega_\Lambda = 0.7$, $h = 0.7$ and $\sigma_8 = 1.0$. For each of the merger trees, we perform 10 realizations of the orbital angular momentum that comes in with each merger. The encounter parameters are taken to be those of typical encounters in simulations, and the directions of the added spins are drawn at random, allowing for a slight correlation between the planes of successive mergers (as seen in simulations, e.g. Dekel et al. 2001; Porciani et al. 2001). We end up with a distribution of 5000 spin values for each halo mass. This distribution is shown in Fig. 4, in comparison with the log-normal distribution obtained by BD from a cosmological simulation. The model predictions of $\lambda'_0 = 0.036$ and $\sigma_\lambda = 0.53$ match rather well the simulated results. One can see in Figure 2 of Maller et al. (2002) that the match is reasonable even without introducing any correlation between the encounter planes.

Similar results were obtained by Vitvitska et al. (2001), who draw their encounter parameters statistically from the distribution found in N-body simulations, and by Monaco, Theuns & Taffoni (2002), where encounter parameters for each object are provided by Lagrangian perturbative theory. We conclude that the simple orbital-merger model is successful in reproducing the simulated halo spin distribution, and therefore serves as a useful tool for studying the angular-momentum buildup in galaxies.

2.2 Modeling the Angular-Momentum Profile

The cumulative mass distribution of specific angular momentum within simulated dark halos, $M(< j)$, was found by BD to be well fit by the 2-parameter universal functional form

$$\frac{M(< j)}{M_{\text{vir}}} = \frac{\mu j/j_{\text{max}}}{\mu - 1 + j/j_{\text{max}}}, \quad \mu > 1, \quad (4)$$

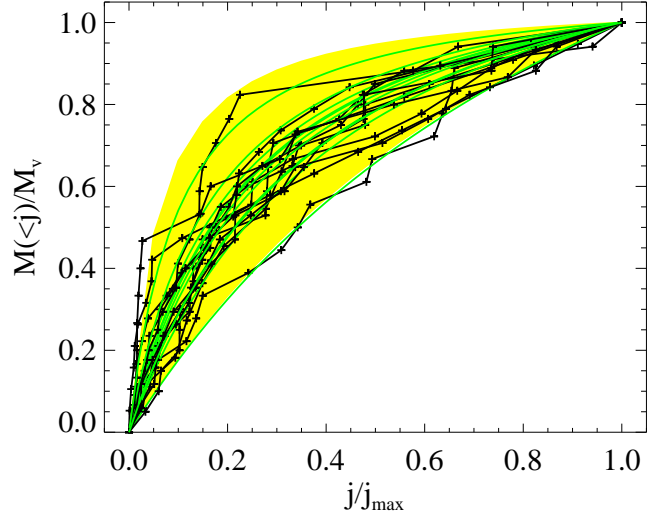


Figure 1. Dark-halo angular-momentum profiles: The mass fraction with specific angular momentum less than j as a function of j/j_{max} . The lines connecting symbols represent a random sample of profiles produced by our orbital-merger model. The smooth curves are fits to these profiles, where μ is chosen to cross at half the total mass. The shaded region marks the 90% spread of profiles found by BD in simulations.

in which one of the parameters, say j_{max} , can be replaced by λ' . This profile is a simple power law, $M(< j) \propto j$, for at least half the mass. When μ is close to unity, it bends over towards the high- j end. The distribution of the shape parameter μ was found to be Gaussian in $\log(\mu - 1)$, with a mean of -0.6 and standard deviation of 0.4 .

One can also quantify the shape of the angular momentum profile by the ratio of the total specific angular momentum, j_{tot} , to j_{max} . The relation between this parameter and μ is

$$\zeta = \frac{j_{\text{tot}}}{j_{\text{max}}} = 1 - \mu(1 - (1 - (\mu - 1) \log \frac{\mu}{\mu - 1})) \quad (5)$$

(BBS eqn. 12).

We create $M(< j)$ profiles for each of the realizations of the orbital-merger model as follows. We divide the mass growth of the halo into 20 equal-mass bins and assign to each bin the corresponding angular momentum that comes in with that mass. When a satellite’s mass is divided among several bins, $i = 1, n$, with a fraction f in bin 1, we assign a fraction f^2 of its angular momentum to bin 1. The remaining satellite mass and angular momentum are then distributed in an analogous way among bins $i = 2, n$. This mimics an $M(< j) \propto j^{1/2}$ profile for the contribution of each satellite, in rough agreement with the predictions of a toy model based on dynamical friction and tidal stripping for an NFW halo (BD; Dekel et al. 2001). The role of this procedure is to smooth the profile; in most cases it does not change the global shape, which is predominantly determined by the cosmological sequence of mergers. The result is therefore not too sensitive to the exact assumed distribution of j due to each single merger.

Fig. 1 shows a sample of j profiles produced by this procedure. Our profiles are somewhat noisier than those seen in simulations, partly because we ignore any exchange of an-

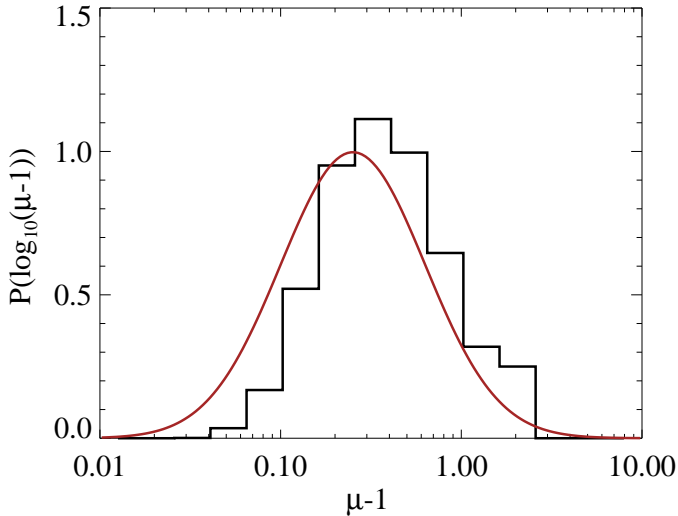


Figure 2. The distribution of shape parameter μ for halo angular-momentum profiles. The histogram describes the distribution in the sample reproduced by our orbital-merger model. The smooth curve is the log-normal fit to the N-body simulation results of BD. There is a slight offset in the mean of the distribution of our model (-0.5 instead of -0.6) but this is not statistically significant.

gular momentum between particles. The overall agreement between our model profiles and the simulation results of BD suggests that the rearrangement of angular momentum only smoothes the profile without changing its global shape. We fit each of our profiles to eq. (4) by the simple method of requiring an exact match at half the virial mass (Fig. 1). The same results follow if we use ζ to compute μ by inverting eqn. 5. We obtain a distribution of μ values that are consistent with the results of BD (Fig. 2). As in BD, they show no dependence on halo mass or redshift. Thus, the orbital-merger model, which reproduces the correct distribution of spin values among halos, also recovers reasonably well the angular-momentum profile inside halos.

Our orbital-merger model reveals an important feature in the buildup of halo angular momentum. We see in the typical realization that the final halo spin and its direction are predominantly determined by one last major merger. Most of the high- j mass in the final distribution comes in with this merger. The many smaller satellites, each possibly carrying a high j , come in at different directions and therefore tend to sum up to a low spin. Thus, most of the low- j fraction of the halo mass originates in minor mergers. This feature provides an important clue for a possible solution to the spin crisis, as follows. If small satellites lose a large fraction of their gas before they merge into the halo then the final gas distribution in the galaxy lacks the low j material. Furthermore, if more of the galactic gas originates in big satellites then the spin of the baryonic component may be higher than that of the dark matter.

3 REPRODUCING THE ANGULAR MOMENTUM CATASTROPHE

3.1 Tidal Stripping and Dynamical Friction

We can understand the transfer of angular momentum from the baryons to the dark matter in cosmological hydrodynamical simulations with a simple model including gas cooling, dynamical friction and tidal stripping. In our model for halo spin buildup discussed above we have not specified how the orbital angular momentum of the satellite is converted to the spin of the halo. Clearly the transfer of angular momentum occurs by the processes of dynamical friction and tidal stripping. The dynamical friction acting by the halo particles on the bound part of the satellite exerts a torque which transfers angular-momentum from the satellite to the halo and eventually brings the satellite towards the halo center. Satellite particles that are tidally stripped and become part of the halo before the satellite sinks to the halo's center retain what is left of their angular momentum at that point and add it directly to the halo.

A hint for the typical $M(< j)$ distribution due to a single merger can be obtained as follows (BD; Dekel et al. 2001). If the satellite moves with a circular velocity $V_c(r)$, and we assume that the lost mass and j are deposited, on average, locally at r , then the resultant spatial profile $j(r)$ can be obtained by averaging over shells,

$$4\pi r^2 \rho(r) j(r) = m(r) \frac{d[rV_c(r)]}{dr} + \frac{dm(r)}{dr} r V_c(r). \quad (6)$$

The first term refers to the J transfer as a reaction to dynamical friction, and the second is the J deposit associated with the tidal mass transfer. We need to estimate the momentary surviving satellite mass $m(r)$ in order to compute $j(r)$, which can then be inverted to obtain the desired $M(< j)$.

The tidal mass loss at halo radius r can be crudely estimated by evaluating the tidal radius ℓ_t of the satellite at r using the crude resonance condition,

$$m(\ell_t)/\ell_t^3 = M(r)/r^3, \quad (7)$$

where $m(\ell)$ and $M(r)$ are the mass profiles of the satellite and halo respectively (e. g. Weinberg 1994). If, for simplicity, these two profiles are *self-similar*, then the resonance condition implies

$$\ell_t/\ell_{\text{vir}} = r/R_{\text{vir}}, \quad (8)$$

where ℓ_{vir} and R_{vir} are the virial radii of the satellite and the halo respectively. This means that the remaining bound mass of the satellite when it is at r obeys

$$m[\ell_t(r)] \propto M(r). \quad (9)$$

A more accurate recipe for tidal stripping, based on studies with N-body simulations of mergers, reveal that eq. (9) is valid as a crude approximation for a wide range of merger parameters (Dekel et al., in preparation). We therefore adopt it in our model.

If the halo density profile is isothermal, $M(r) \propto r$, then substituting eq. (9) in eq. (6) yields $j(r) \propto r$, which corresponds to $M(< j) \propto j$. A more realistic NFW density profile leads in the outer halo to a j profile closer to $M(< j) \propto j^{1/2}$, (BD; Dekel et al. 2001) which is what we use to smooth the profile in the orbital-merger algorithm. The qualitative similarity between the profile predicted by this toy model and the typical j profile seen in simulations (BD) provides further support to the general picture of J buildup by mergers.

3.2 Spin Segregation

We can now explore the effect of cooling in the satellites on the final angular momentum of the baryons. We assume that at an early time the baryons follow the dark-matter distribution. As the gas within a halo cools radiatively, it contracts to a more compact configuration characterized by a smaller radius, R_b , compared to the extent of the dark matter, R_{dm} . Such a spatial segregation in a satellite before it merges with a bigger halo naturally leads to a difference in the spins of baryons and dark matter in the product halo. The bound part of the satellite is continuously transferring orbital angular momentum to the dark matter by dynamical friction. In the extreme case, the inner satellite that remains bound all the way to the halo center eventually loses all its orbital angular momentum by this mechanism. At the moment of stripping, the escaping satellite material stops being affected by dynamical friction, and it joins the halo with the angular momentum that it is left with at that point.

The spatial segregation in the satellite thus implies that the j -rich mass stripped at the early stages of the merger in the outer halo is dominated by dark matter, while the more compact baryonic component survives longer as a bound satellite and loses more of its orbital angular momentum by dynamical friction. The result is a net transfer from the baryons to the dark-matter component. This process is illustrated in a schematic diagram, Fig. 3.

Using eqn. 8 above, we obtain that the orbital angular momentum added to the merger product with the baryons is related to the amount gained by the dark matter via

$$\Delta J_b = \frac{R_b}{R_{dm}} \Delta J_{dm}. \quad (10)$$

We ignore any transfer of angular momentum from the satellite to the baryons already in the halo as baryons in the more massive halo are already more centrally concentrated than those in the satellite. In the case of maximum cooling the baryons dominate the center of the halo which we approximate as $R_b = f_b R_{dm}$, where f_b is the universal baryon fraction. Adopting $f_b = 0.13$ (Tytler et al. 1999), we obtain that the spin of the baryons is reduced by almost an order of magnitude, and thus reproduces the angular momentum catastrophe as seen in hydrodynamical cosmological simulations. In Fig. 4 we show the resultant probability distribution of the spin parameter as obtained in our orbital-merger model with maximum cooling; it has $\lambda'_0 = 0.005$.

This simple modeling of the spin problem makes it easy to understand why it is usually assumed that some form of energy input into the gas may remedy the problem; it would delay the cooling, increase R_b , and thus reduce the baryonic spin loss.

Note that in common semi-analytic models of galaxy formation the gas is assumed to be either in a hot phase or in a cold phase, with the hot phase extending out to R_{dm} and the cold phase condensed. This implies that the cold gas in the satellite loses most of its angular momentum to dynamical friction, while the hot gas retains most of its angular momentum. In this case the fraction of baryons in the hot phase, f_{hot} , determines the orbital angular momentum added as baryonic angular momentum to the merger product, $\Delta J_b = f_{hot} \Delta J_{dm}$. Thus, one can relate our discussion here to other semi-analytic modeling by identifying $f_{hot} = R_b/R_{dm}$.

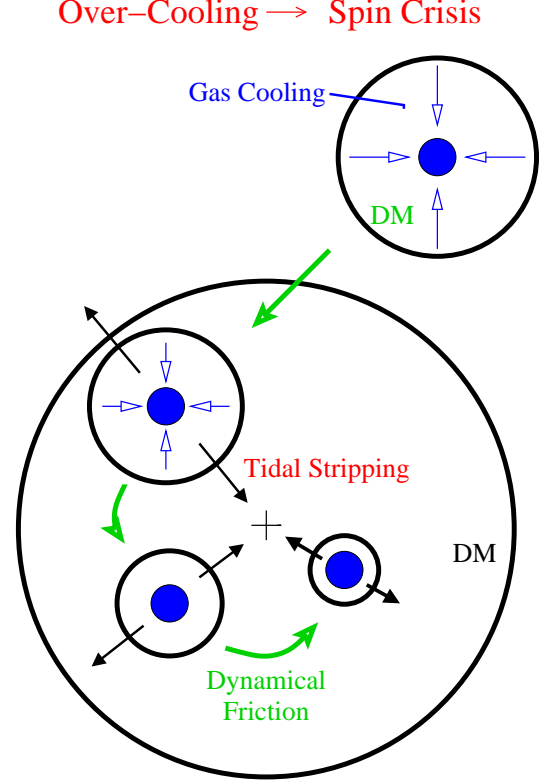


Figure 3. A schematic illustration of how over-cooling in merging satellites leads to the angular momentum catastrophe. The gas contraction within the incoming satellite makes the gas immune against tidal stripping: it spirals all the way into the halo center while losing all of its orbital angular momentum to the dark halo due to dynamical friction. The dark matter, which dominates the outer regions of the satellite, is gradually stripped in the outer parts of the halo, thus retaining part of its orbital angular momentum.

4 FEEDBACK

It is generally assumed that some form of heating may play an important role in preventing over-cooling and therefore angular-momentum loss. The most important source of heating is likely to be supernova feedback though reionization by the UV background, tidal heating, and ram pressure may all contribute. Semi-analytic models assume different ad hoc recipes for the amount of heating as a function of star-formation rate, though hydrodynamical simulations have been largely unsuccessful so far in implanting feedback in a way that prevents over-cooling (see Thacker & Couchman 2000, and references therein). Our approach in the present work is to avoid the details of star formation and feedback recipes and rather use a very simple prescription for the effect of feedback in a satellite halo as a function of its virial velocity, V_{sat} .

Following the analysis in §IV of DS, we assume that the total supernova energy pumped into the gas per unit mass is a robust quantity. This is based on the assumptions that the supernova rate is roughly proportional to the same gas mass that is later being affected by it, that the star-formation rate is inversely proportional to the dynamical time, and that

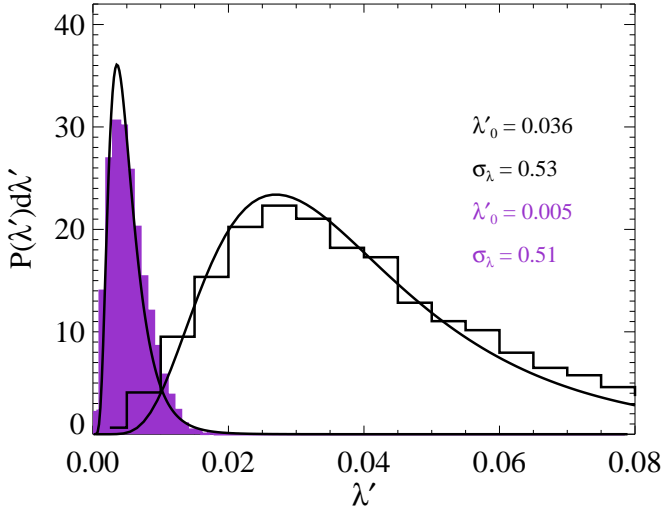


Figure 4. The effect of over-cooling on the spin distribution of baryons compared to the dark matter. Since the baryons are tightly bound in the satellite centers, they spiral into the inner part of the big halo without being stripped and thus lose most of their angular momentum to the halo by dynamical friction. The model reproduces the deficiency of angular momentum in baryons of almost an order of magnitude as seen in hydrodynamical simulations.

the supernova remnant transfers most of its energy to the interstellar medium by the end of its “adiabatic” phase. DS estimated as a crude upper limit that the supernova input is comparable to the kinetic energy per unit mass of an isothermal halo with virial velocity $\sim 100 \text{ km s}^{-1}$. The actual free parameter characterizing our feedback model, V_{fb} , is defined as the virial velocity of a halo for which the energy input is sufficient to heat all the gas to the virial temperature of the halo. Based on DS we expect V_{fb} to be of order 100 km s^{-1} or less, but we keep this estimate in mind only as a general constraint which does not enter our current analysis. The actual relation between V_{fb} and the supernova input depends on the initial state of the gas before the supernova burst.

We thus parameterize the effect of feedback on the spatial extent of the baryons in a halo by the ratio of V_{sat} to V_{fb} . The limit $V_{\text{sat}} \gg V_{\text{fb}}$, massive halos with deep potential wells, corresponds to maximum cooling, $R_{\text{b}} \ll R_{\text{dm}}$. For smaller halos with $V_{\text{sat}} \simeq V_{\text{fb}}$ we expect the heating to balance the cooling and yield $R_{\text{b}} \simeq R_{\text{dm}}$. Our model is therefore a simple interpolation between these limits,

$$R_{\text{b}} = \left(\frac{V_{\text{fb}}}{V_{\text{sat}}} \right)^{\gamma_1} R_{\text{dm}} \quad (V_{\text{sat}} > V_{\text{fb}}), \quad (11)$$

with γ_1 an arbitrary exponent.

If V_{fb} is larger than V_{sat} , the feedback can cause gas ejection from the satellite. For $V_{\text{sat}} \ll V_{\text{fb}}$ we expect total blowout, and we assume that partial blowout starts occurring for halos where the potential energy of the gas is comparable to the energy input from supernova, $V_{\text{sat}}^2 = (1/2)V_{\text{fb}}^2$. We therefore parameterize the amount of gas that remains in the halo by another simple interpolation,

$$f_{\text{d}} = \left(\frac{V_{\text{sat}}}{\sqrt{2}V_{\text{fb}}} \right)^{\gamma_2} \quad (V_{\text{sat}} < V_{\text{fb}}/\sqrt{2}), \quad (12)$$

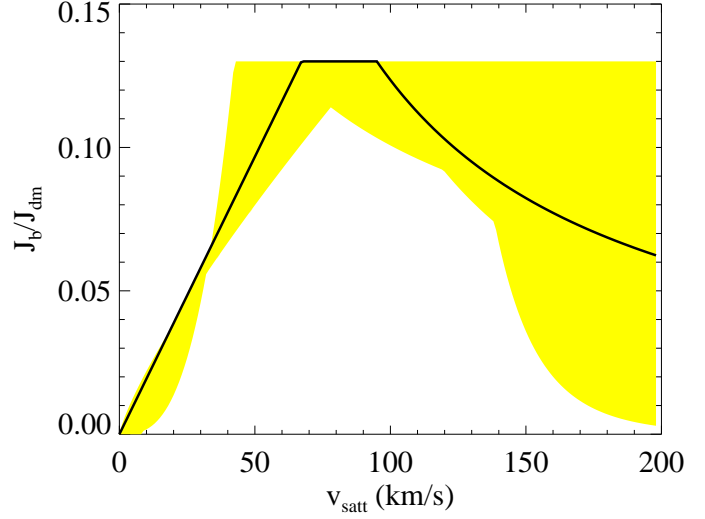


Figure 5. The effect of feedback on the ratio of baryonic angular momentum to that of the dark matter as a function of the virial velocity of the merging satellite. In the model described by the thick curve, the feedback is characterized by $V_{\text{fb}} = 95 \text{ km s}^{-1}$, with the exponents $\gamma_1 = \gamma_2 = 1$. If the baryons in the satellite are distributed like the dark matter (middle range), then $J_{\text{b}}/J_{\text{dm}} = f_{\text{b}}$, the cosmological baryon fraction. In larger satellites with $V_{\text{sat}} > V_{\text{fb}}$, the baryons are less extended than the dark matter and thus lose more angular momentum by dynamical friction before they are stripped into the halo. In smaller satellites with $V_{\text{sat}} < V_{\text{fb}}/\sqrt{2}$, gas is blown out and therefore J_{b} is reduced, though the specific angular momentum of the baryons remains the same as that of the dark matter. The shaded region shows the range of models we consider in § 6, all constrained to match the baryonic fraction in dwarf galaxies.

with γ_2 another arbitrary exponent.

We start with the simplest arbitrary choice $\gamma_1 = \gamma_2 = 1$. Later, in section 6, we will explore the robustness of the results to different assumptions about choices of values for γ_1 and γ_2 .

The only remaining free parameter of the feedback model is V_{fb} . We set it by requiring that halos with a virial velocity of 60 km s^{-1} have an average $f_{\text{d}} = 0.04$, as measured in the data of BBS. Note that we are concerned with the state of the baryons only when the satellite merges with the halo; it is therefore sufficient that the feedback be effective for a short duration, perhaps triggered by the merging process itself.

The effects of heating and blowout on the angular momentum of baryons versus dark matter, according to our model, is shown in Figure 5. For massive satellite with $V_{\text{sat}} > V_{\text{fb}}$, the baryons retain less angular momentum as the mass increases, because of dynamical friction. Small satellites with $V_{\text{sat}} < \sqrt{2}V_{\text{fb}}$ allow a blowout of a larger fraction of their gas as the mass decreases, thus adding to the merger product less baryons and therefore less baryonic angular momentum, while the specific angular momentum of the two components remains the same.

In Fig. 6 we demonstrate the effects of the different ingredients of this feedback scheme, with $V_{\text{fb}} = 95 \text{ km s}^{-1}$, on the baryonic spin-parameter distribution. We do it for two kinds of final halo masses, corresponding to virial velocities

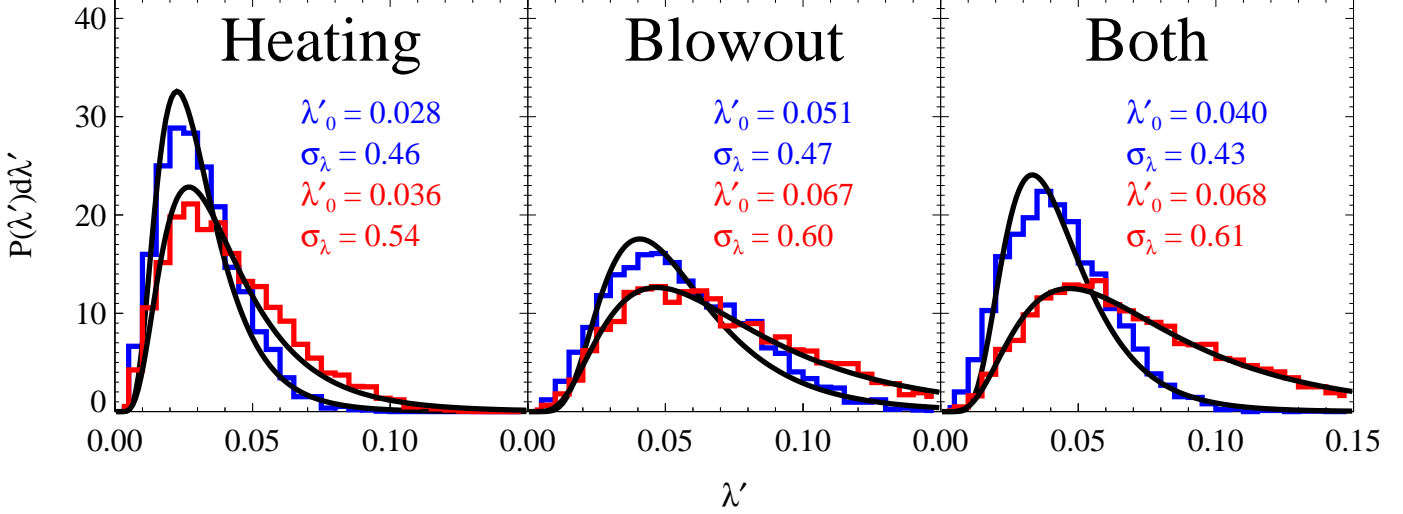


Figure 6. The effects of heating and blowout in our model on the distribution of baryonic spin parameter λ' . Log-normal fits are shown for each histogram, with the corresponding mean and scatter quoted. In each panel the higher peaked curve and higher two numbers are the bright galaxies ($V_{\text{vir}} = 220 \text{ km s}^{-1}$) and the lower peaked curve and lower two numbers are the dwarf galaxies ($V_{\text{vir}} = 60 \text{ km s}^{-1}$). **Left:** Only heating is included in our feedback recipe (blowout ignored). **Center:** Only blowout is included (cooling ignored). **Right:** The whole feedback recipe is included, with cooling, heating and blowout.

of 60 and 220 km s^{-1} . We refer to these as representing *dwarf* and *bright* galaxies respectively.

The left panel of Fig. 6 shows the effects of adding heating only, ignoring blowout. The dwarf galaxies are all built up by satellites of $V_{\text{sat}} < V_{\text{fb}}$, so there is full heating, $R_b \simeq R_{\text{dm}}$. The result is that the spin distribution of the baryons resembles that of the dark-matter. In bright galaxies, the partial heating raises the baryonic spin to $\lambda'_0 = 0.028$, which is still lower than the typical spin of the dark matter due to the partial cooling.

The center panel shows the effects of full heating ($R_b \simeq R_{\text{dm}}$) and blowout, as if there is no cooling. For the two kinds of galaxies, the baryonic λ' distribution becomes significantly higher than that of the dark matter, with $\lambda'_0 = 0.051$ for the bright galaxies and a very high $\lambda'_0 = 0.067$ for the dwarf galaxies.

Finally, the right panel shows the result of applying the full feedback scheme, considering cooling, heating and blowout together. The baryons in the bright galaxies now have spins comparable and even slightly higher than their dark-matter halos, with $\lambda'_0 = 0.040$ (and $\sigma_\lambda = 0.43$), while the baryons in dwarf galaxies now have spins higher by $\sim 50\%$, with $\lambda'_0 = 0.068$ (and $\sigma_\lambda = 0.61$).

Thus, the baryonic spin in dwarf galaxies, which are made by mergers of small satellites, is dominated by the blowout of the gas from these satellites, and it ends up with $\lambda'_b > \lambda'_{\text{dm}}$. For bigger galaxies, which are largely made of bigger satellites, the dominant effect preventing the over-cooling spin catastrophe is the heating, with some contribution from blowout. This yields a baryonic spin distribution similar to that of the dark matter halos, in general agreement with observations.

5 MODEL VERSUS OBSERVATIONS

We now confront the model predictions with observations, in particular those of BBS. We first calibrate the value of the one free parameter V_{fb} by the observed gas deficit in dwarf galaxies. We then address the distribution of the baryonic spin parameter in these galaxies, as well as the angular momentum profiles within dwarf and bright disks.

5.1 Observations

Generally, galaxy formation modelers have compared their predicted disk sizes to the distribution of disk scale lengths found in large samples of late type galaxies (Courteau 1996; Mathewson et al. 1992). A more detailed comparison has been performed by de Jong & Lacey (2000) where they constructed the bivariate space density of galaxies as a function of luminosity and size. This allows the spread in observed disk sizes to be compared to models and they found that the spread corresponded to a σ_λ of only 0.36 ± 0.03 . Ideally one would like to compare the actual angular momentum in models with observed galaxies instead of just properties derived from the angular momentum.

The only observational attempt so far to measure spin parameters for galactic disks is by BBS, which therefore serves as the main target for our modeling effort in this paper. BBS used fits to the rotation curves and assumed an NFW profile for the halos (Navarro et al. 1995) in order to determine the halo virial quantities R_{vir} and V_{vir} for 14 dwarf galaxies, with an average $V_{\text{vir}} \simeq 60 \text{ km s}^{-1}$. They also assumed a mass-to-light ratio of unity in the R band, but their results are not very sensitive to this assumption because dwarf galaxies are dominated by their dark matter halos. BBS then determined for each galaxy the baryonic

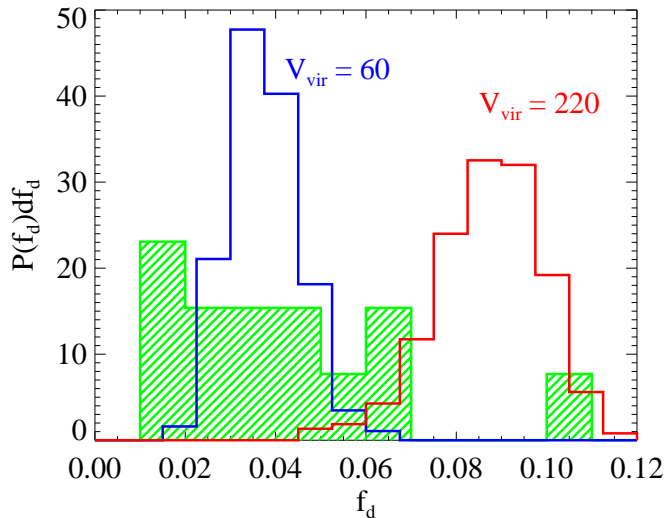


Figure 7. The probability distribution of the fraction of mass in baryons f_d for the data of BBS (shaded), in comparison with our model predictions with $V_{fb} = 95 \text{ km s}^{-1}$ for dwarf galaxies (left) and for bright galaxies (right). The model prediction for the dwarf galaxies, with significant blowout, is in good agreement with the BBS data. The bright galaxies retain most of their baryons.

spin parameter λ_b which we have converted to λ'_b using their values for c_{vir} and equation 2. This leads to an average value of $\lambda'_b \simeq 0.063$, significantly larger than that of simulated dark-matter halos. They also estimated the ratio f_d of disk mass (stars + gas) to dark-matter mass, and found an average of $f_d \simeq 0.04$, about a factor of 3 smaller than the universal baryonic fraction (Tytler et al. 1999). Finally, they measured the j distribution in each galaxy, and confirmed the mismatch of angular-momentum profiles. We discard one galaxy (UGC4499) from the sample because its rotation-curve fit yields strikingly anomalous results.

5.2 Baryon Fraction

The distribution of f_d values for the dwarf galaxies of BBS is displayed in Fig. 7 as a shaded histogram. These values are significantly lower than the generally adopted universal value of $f_b \simeq 0.13$, which suggests significant baryonic mass loss from these objects. Shown for comparison are the corresponding model predictions for dwarf and bright galaxies. We have chosen a value of $V_{fb} = 95 \text{ km s}^{-1}$ in order to match the mean of the BBS measurements for dwarf galaxies, $f_d \simeq 0.04$, but one can see in Fig. 7 that the resulting spread in f_d values is also in good agreement with the dwarf galaxies data. For bright galaxies, f_d is typically lower than the universal value by only $\sim 30\text{--}40\%$, reflecting the limited fraction of small merging satellites who lost their gas.¹ It is

¹ There is one dwarf galaxy with an f_d value much higher than the rest of the distribution. This galaxy has the lowest virial velocity in the sample, $V_{vir} = 43 \text{ km s}^{-1}$, and the second highest concentration parameter, $c_{vir} = 31$, suggesting that there may be something unusual about this galaxy, either in its history or in the BBS fit to its rotation curve.

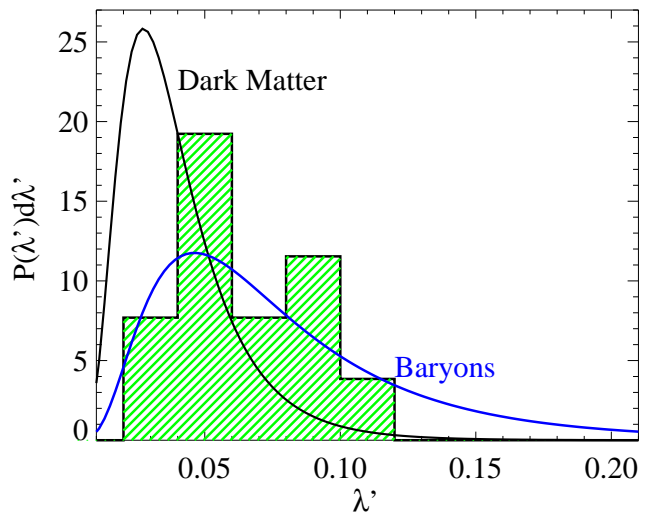


Figure 8. The distribution of λ' in the sample of dwarf galaxies by BBS (shaded histogram) compared with our model predictions with $V_{fb} = 95 \text{ km s}^{-1}$ for the baryons in dwarf galaxies (curve on the right), and the simulation result for dark halos by BD (curve on the left). The inclusion of blowout produces a λ' distribution in good agreement with the data.

encouraging that the obtained value for V_{fb} is in the range of expected values for supernova-driven winds (DS).

5.3 Spin Parameter of Baryons

Next, we compare predicted and observed distributions of spin parameters for dwarf galaxies. The distribution of λ'_b for the BBS disks of dwarf galaxies is plotted in Figure 8 as a shaded histogram. Shown first in comparison is the λ' distribution for dark halos in cosmological Λ CDM simulations from BD. Contrary to comments made by BBS, these two distributions are not in agreement — the observed spins are significantly higher, with an average of 0.063 compared to 0.035 in the dark-matter simulations. Finally shown in Figure 8 is our model prediction for the baryonic spin distribution in dwarf galaxies ($V_{vir} = 60 \text{ km s}^{-1}$), with $V_{fb} = 95 \text{ km s}^{-1}$. The effect of blowout brings the baryonic spin distribution into good agreement with the observed sample. Note that this distribution is quite different than that of the dark matter, with $\lambda'_0 = 0.068$ and $\sigma_{\lambda} = 0.61$. We find it remarkable that the agreement with the observed spin distribution follows automatically from the adjustment of V_{fb} to match the observed baryonic fraction in dwarf galaxies. In the next section we demonstrate that the result is also independent of the details of the feedback model used.

In the context of the scatter issue mentioned above we note that the predicted spread in λ' values for baryons in bright galaxies is smaller than the spread for the dark-matter halos ($\sigma_{\lambda} = 0.43$ versus 0.5), and is more like the spread observed by de Jong & Lacey (2000). We note also that the high baryonic spin values obtained in our model for both dwarf and bright disks suggests that one does not need to eliminate low-spin halos in order to match the observed distribution of disk sizes [e.g., as done in Mo et al. (1998)].

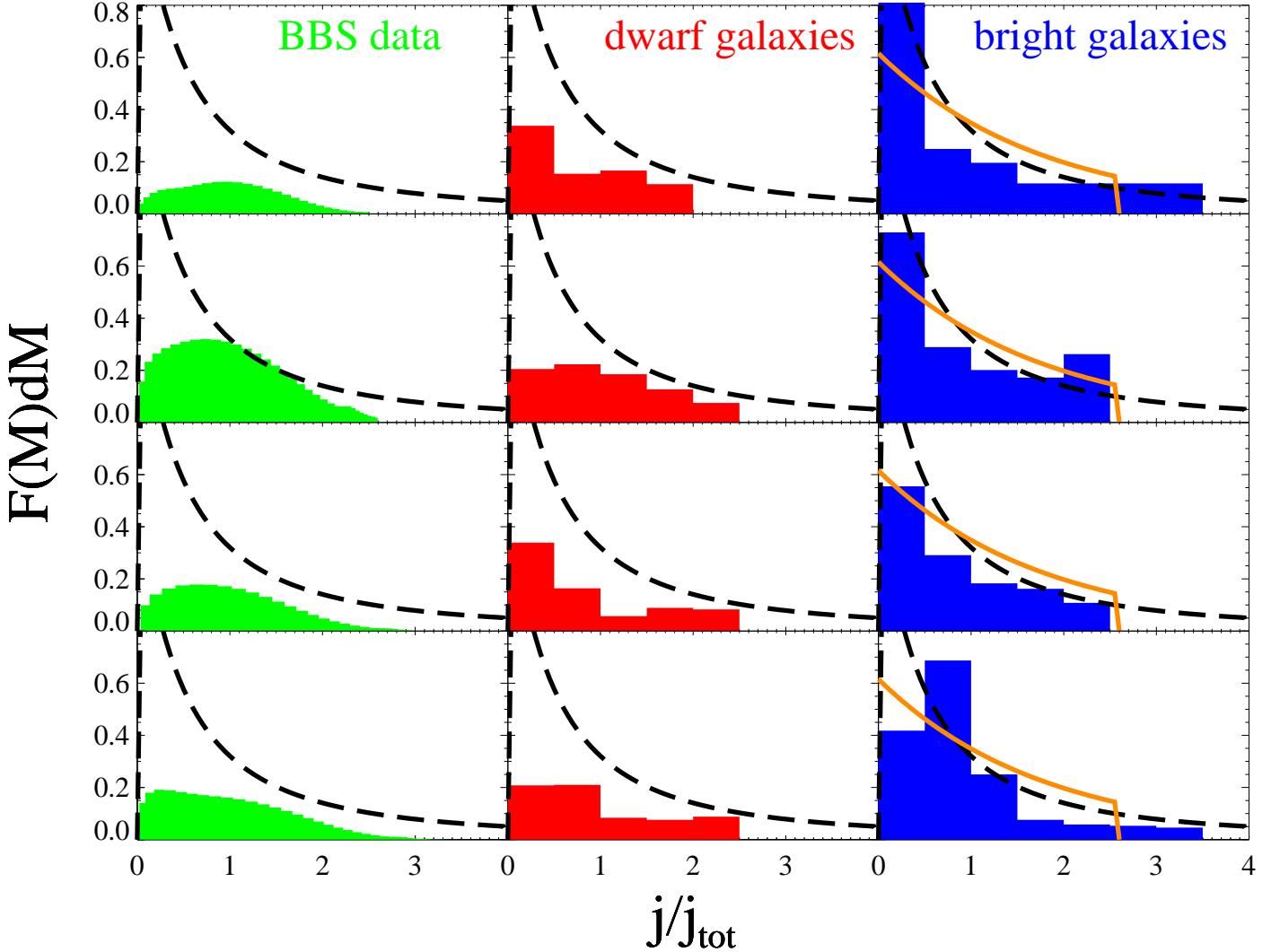


Figure 9. Examples of baryonic specific angular-momentum profiles for the BBS data (left column) and for our model dwarf and bright galaxies (center and right columns respectively). Also drawn is the average ($\mu = 1.25$) dark-matter j -profile seen in the simulations of BD (dashed curve). The BBS profiles clearly lack the high and low j tails seen in the simulations. Likewise, many of our model dwarf galaxies also lack this material because of gas loss. The bright galaxies, which retain most of their baryons, have j profiles more similar to the dark matter. However, in some cases they are consistent with the profile of an exponential disk with a flat rotation curve (solid curve in right column).

5.4 Angular-Momentum Profile of Baryons

BBS also measured the specific angular momentum profiles of their dwarf galaxies, which they find to be quite different from the profiles of dark halos found by BD. The dwarf galaxies in their sample show a systematic behavior, with a low baryonic fraction, and a significant deficit of angular momentum at the two ends of the distribution compared to the halo j profiles of BD. Examples of some of the j profiles from their data are shown in the left column of Fig. 9.

We construct a baryonic j profile in each of our model realizations, following the same method used to produce dark-matter j profiles in §2.2, but now including feedback and gas loss. Examples of such model profiles for dwarf galaxies of $V_{\text{vir}} = 60 \text{ km s}^{-1}$ are shown in the central column of Fig. 9. The low- j tail of the halo distribution is missing in the baryons in many cases, as expected, because

the blowout preferentially removes gas from small satellites — those satellites that merge to form the low- j halo material. The high- j tail tends to be reduced in the baryons, because this tail is often the result of a small satellite that comes in with its orbital angular momentum aligned with the halo spin, and now has lost its gas. While there is general agreement between the model dwarf galaxies and the BBS data, sometimes the model galaxies show a spike of low j material that is not seen in the data. We can think of several alternative reasons for this apparent discrepancy. Either the predicted spike corresponds to a baryonic component that BBS fail to observe (such as faint halo stars), or these galaxies which show a spike do not become disk dwarf galaxies and are therefore missing from the BBS sample, or our model is missing a certain element that should eliminate the very low- j spike more efficiently.

The right column of Fig. 9 shows the model predictions

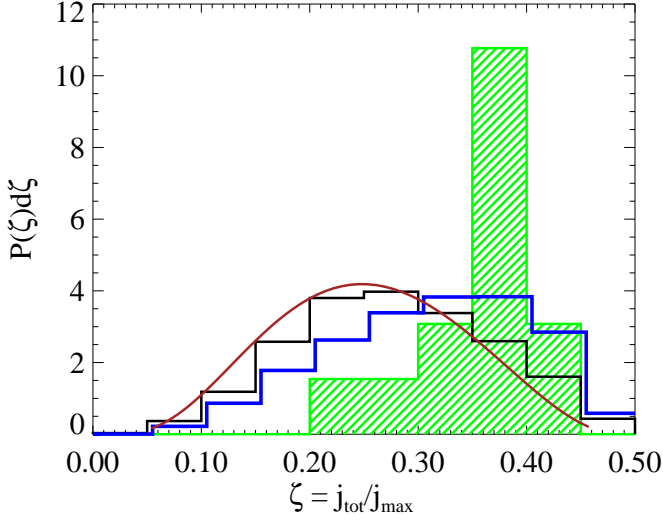


Figure 10. Probability distribution of the spin-profile shape parameter $\zeta = j_{\text{tot}}/j_{\text{max}}$ (the BBS alternative to μ of BD) for the dwarf-galaxy data of BBS (shaded histogram) in comparison with our model predictions for the baryons in dwarf (thick histogram) and bright (thin histogram) galaxies. Shown also is the result for simulated halos by BD (smooth curve). The model prediction for baryons is in reasonable agreement with the data, though the predicted spread is somewhat larger. Bright galaxies show a slightly shifted distribution to higher values of ζ .

for a sample of bright galaxies, $V_{\text{vir}} = 220 \text{ km s}^{-1}$. They retain most of their baryons, so their profiles are less affected by blowout, and they are more similar to the dark-matter j -profiles seen in the simulations of BD. However, in some cases they show a reduction of both low and high j material for the same reasons that it is seen in the dwarf galaxies. For comparison, we also show in the right column of Fig. 9 the j profile of an exponential disk with a flat rotation curve truncated at 4.5 disk scale lengths. The j -profile mismatch problem in bright galaxies is partly remedied by the common presence of low- j bulge components in such galaxies. The fact that sometimes the low- j material is lost even from bright galaxies allows some of them to become pure exponential disks, as observed, without the need to hide any low- j material in a bulge.

Fig. 10 shows the distributions of the quantity ζ , which characterizes the shape of the j -profile. It compares the observed values in the BBS dataset with our model predictions for the baryons in dwarf and in bright galaxies. Given the crudeness of our model, the agreement between our model for dwarf galaxies and the data is quite reasonable. The somewhat smaller spread in the data compared to the model predictions may suggest that either selection effects or gas processes tend to favor a particular value of ζ . Also shown for comparison is the distribution of ζ for dark halos as measured by BD in simulations. One sees that the values of ζ for bright galaxies are slightly shifted to higher values than the dark halos. For dwarf galaxies the shift is a significant effect, reflecting the mismatch between the j -profiles of dark halos and observed galaxies.

Table 1. The dependence of our results on the model parameters. For a given γ_2 the scale V_{fb} is set by requiring the average f_d in dwarf galaxies ($V_{\text{vir}} = 60 \text{ km s}^{-1}$) to be 0.4. Then we find the lowest value of γ_1 that creates a spin distribution in bright galaxies ($V_{\text{vir}} = 220 \text{ km s}^{-1}$) with a median ≥ 0.035 .

γ_2	model		dwarf galaxies			bright galaxies		
	V_{fb}	γ_1	f_d	λ'_0	σ_λ	f_d	λ'_0	σ_λ
0.5	185	3.0	0.4	0.061	0.56	0.8	0.053	0.50
0.8	130	3.0	0.4	0.063	0.56	0.8	0.035	0.53
1.0	95	1.5	0.4	0.067	0.61	0.9	0.035	0.44
3.0	60	0.5	0.4	0.082	0.64	0.9	0.036	0.42

6 ROBUSTNESS OF THE FEEDBACK MODEL

In this section we examine the sensitivity of our results in the previous section to our extremely simple model of feedback. We explore a range of values for the exponents γ_1 and γ_2 . For each choice of exponents, we determine V_{fb} such that the mean value of f_d for the dwarf galaxies is the same as the BBS value of 0.04. We find that the results of § 5 for dwarf galaxies remain practically unchanged. The results for bright galaxies do depend on the value of γ_1 , though a value can always be chosen such that the median spin for the bright galaxies is at least as high as that of the dark halos.

In Table 1 we show a range of values of γ_2 and the corresponding values of V_{fb} necessary to give our dwarf halos the right baryon fraction f_d . Then we list the largest value of γ_1 for which bright galaxies have a median $\lambda'_b \geq 0.035$, as suggested observationally. A maximum value of 3.0 is considered for both exponents as higher values produce indistinguishable results. The resulting values of f_d , λ'_0 and σ_λ are listed for the two types of galaxies. We indeed see in the table that varying the exponents γ_1 and γ_2 has a small effect on the resulting baryonic spin distribution for dwarf galaxies. We conclude that any feedback recipe in which an appropriate amount of gas is being ejected from dwarf galaxies should resolve the angular-momentum crisis for dwarf galaxies in a way similar to our results in §5. The angular momentum catastrophe for bright galaxies is prevented if γ_1 is sufficiently small.

If γ_2 is as small as 0.5, as in the first row of Table 1, then the required value of V_{fb} needed to fit the mean value of f_d in dwarf galaxies is very high (185 km s^{-1}). This velocity is significantly higher than the crude upper limit allowed by the energetics (DS). Also, for such a large V_{fb} value bright galaxies have a median λ' much higher than the dark matter even for the maximum value of γ_1 . Thus, the model yields sensible results only if γ_2 is limited to the range $0.8 - 3.0$.

The shaded region in Fig. 5 shows the range of curves corresponding to the range spanned in Table 1. We note that a tight constraint is enforced by the data on this range of feedback models, that halos of $\sim 35 \text{ km s}^{-1}$ must lose about half of their baryons.

7 CONCLUSION

We used a simple model to address the two issues that create the angular-momentum crisis of galaxy formation within the CDM scenario. One, the angular momentum catastrophe is that the spin of the baryonic component in galax-

ies is typically comparable to that of the dark-matter halo (in bright galaxies) or even larger (in dwarf galaxies), while simple theoretical arguments and simulations involving gas dynamics predict a significant spin loss by the baryons due to over-cooling in merging halos. The other, the mismatch of angular-momentum profiles, is that the baryons in each galaxy tend to lack the low- j tail (and the high- j tail) of the distribution as predicted by simulations for the dark halos.

In an earlier paper (Maller et al. 2002), we showed that a simple algorithm, based on adding up the orbital angular momenta of the mergers in random realizations of merger histories, can successfully reproduce the distribution of spins among dark-matter halos as measured in N-body simulations of the Λ CDM cosmology. We showed here that an extension of such a model also reproduces the characteristic angular-momentum profile, i.e., the distribution of specific angular momentum within halos. This provided the basic tool for addressing a possible resolution to the spin problems by incorporating the effects of supernova feedback on the gas in halos before they merge into bigger halos — a process we have termed spin segregation.

A simple analysis of how the orbital angular momentum in a merger turns into a spin profile suggested how feedback effects in the satellite before the merger event can eliminate the problem of spin loss. The effective size of the gas component within the incoming satellite determines its tidal stripping position in the halo and thus the final spin that it will be left with after the merger. The finding, using the orbital-merger model, that the low-end tail of the j distribution originates in many minor mergers, that tend to cancel each other's angular momentum, provided a possible solution to the spin-profile mismatch problem. The blowout of gas from small incoming halos would eliminate the low- j tail of the baryon distribution in the merger product, as observed. The blowout has a particular strong effect in dwarf galaxies, because they are made of smaller progenitors that tend to lose more of their gas. This results in a higher spin parameter for the baryons than the dark matter, as observed.

We constructed a simple semi-analytic model for simulating this process using a simplified model for the effects of feedback as a function of halo mass, including heating and blowout. For a given choice of exponent γ_2 , the model has one free parameter, the characteristic halo virial velocity V_{fb} for which the energy inputted to the IGM by supernova is sufficient to counter the effect of cooling. By matching the low baryonic fraction in the dwarf galaxies observed by BBS, we found that for $0.8 \leq \gamma_2 \leq 3$ the characteristic velocity has to be in the range $60 \leq V_{\text{fb}} \leq 130 \text{ km s}^{-1}$, which falls within the range of theoretical predictions (e.g., DS). We then found considerable agreement between the model predictions and the observed data for both the distribution of the spin parameter and the angular-momentum profile of baryons in dwarf and bright galaxies. We also noted that the same basic model may explain the other unresolved issues concerning angular momentum in galaxies, such as the spread in observed disk sizes and the identification of halos that form late type galaxies. The success of the model in matching several independent observations indicates that this simple model indeed captures the main features necessary for a full scenario involving feedback and mergers that can resolve the spin crisis in more detail. The next natural step should be

to incorporate a more sophisticated feedback recipe into the model using the full machinery of semi-analytic models of galaxy formation. This will be a step towards the long-term goal of implementing feedback in full-scale hydrodynamical cosmological simulations.

Our work is an attempt to resolve the angular-momentum problems within the standard framework of CDM cosmology, which is so successful on large scales, using the effects of feedback which we know must occur. Another approach is to appeal to a different cosmological scenario, WDM, where the dark-matter particles are “warm” rather than “cold” (Hogan 1999; Hogan & Dalcanton 2000; Pagels & Primack 1982). WDM is less robust than CDM because it requires fine-tuning of a new parameter, the particle mass, which is constrained to be $\simeq 1 \text{ keV}$. Still, it is worth investigating since it may remedy the angular-momentum problems without appealing to strong feedback effects. The main distinguishing feature of the WDM scenario is that the formation of small halos is significantly suppressed, such that the validity of the explicit picture of halo buildup by the hierarchical build up of small halos becomes limited. Despite this difference from CDM, an N-body simulation of WDM (Bullock et al. 2001) indicates that the angular-momentum properties of halos remain basically unchanged. This is not very surprising because in Maller et al. (2002) we found that the same angular-momentum properties can also be interpreted as a general result of tidal-torque theory, independent of the explicit picture of mergers (see also BD). In the absence of small halos at early times, one may expect less over-cooling in halos before they merge into other halos and thus less angular-momentum loss by the baryons. Indeed, hydrodynamical simulations of this scenario (Sommer-Larsen & Dolgov 2001) indicate that the angular momentum catastrophe is significantly remedied. However, the angular-momentum profile mismatch is still expected to be valid in WDM, and, in the absence of small halos, the feedback effects are weaker and may not be enough for resolving the problem. Thus the j -profile mismatch may be a crucial discriminator between solutions to the problems of CDM.

It is clear that some sort of heating may provide the cure for another problem of CDM, the dwarf satellite problem (Klypin et al. 1999; Moore et al. 1999), where the predicted number of dwarf halos is much larger than the observed number of dwarf galaxies. Bullock et al. (2000) demonstrated that cosmological photo-ionization due to feedback from UV sources such as early stars and quasars can solve this problem. Feedback from supernova would qualitatively have a similar effect. While the number of dwarf satellites is automatically suppressed in WDM, it seems that the inclusion of minimum realistic feedback effects would reduce the predicted number of galaxies to significantly below the observed number, and thus be an overkill (J. Bullock, private communication).

Furthermore, it is becoming clear (Dekel et al., in preparation) that the key elements of our model, namely the tidal effects in mergers and the feedback effects in small halos, are also very relevant in understanding and resolving the third problem of CDM. This is the cusp/core problem, where the halos in simulations typically show steep cusps in their inner profiles (Navarro et al. 1995; Moore et al. 1999), while observations indicate flat cores at least in some low-surface-brightness galaxies (de Blok et al. 2001). An analysis of tidal

effects explains the necessary formation of an asymptotic cusp in halos as long as satellites continue penetrating into the halo center. Feedback effects may puff up small satellites and prevent them from penetrating the core, thus allowing a stable core. These studies together indicate that our model indeed grasps the relevant elements of the complex processes involved, and that feedback effects may indeed provide the cure to all three major problems of galaxy formation in CDM.

This research has been supported by the Israel Science Foundation grant 546/98, by the US-Israel Binational Science Foundation grant 98-00217, and by the German-Israeli Science Foundation grant I-629-62.14/1999. We thank James Bullock and Frank van den Bosch for stimulating discussions. We also thank Frank van den Bosch for providing us with the BBS data in Fig. 9.

REFERENCES

- Bond J. R., Cole S., Efstathiou G., Kaiser N., 1991, *ApJ*, 379, 440
- Bullock J. S., Dekel A., Kolatt T. S., Kravtsov A. V., Klypin A. A., Porciani C., Primack J. R., 2001, *ApJ*, 555, 240 (BD)
- Bullock J. S., Kravtsov A. V., Colin P., 2001, *ApJL*, submitted, astro-ph/0109432
- Bullock J. S., Kravtsov A. V., Weinberg D. H., 2000, *ApJ*, 539, 517
- Courteau S., 1996, *ApJS*, 103, 363
- de Blok W. J. G., McGaugh S. S., Rubin V. C., 2001, *AJ*, 122, 2396
- de Jong R. S., Lacey C., 2000, *ApJ*, 545, 781
- Dekel A., Porciani C., Kolatt T. S., Bullock J. S., Kravtsov A. V., Klypin A. A., Primack J. R., 2001, in *ASP Conf. Ser. 230: Galaxy Disks and Disk Galaxies*, pp 565–572
- Dekel A., Silk J., 1986, *ApJ*, 303, 39 (DS)
- Eke V., Efstathiou G., Wright L., 2000, *MNRAS*, 315, L18
- Fall S. M., Efstathiou G., 1980, *MNRAS*, 193, 189
- Ferrara A., Tolstoy E., 2000, *MNRAS*, 313, 291
- Gardner J. P., 2001, *ApJ*, 557, 616
- Hogan C. J., 1999, astro-ph/9912549
- Hogan C. J., Dalcanton J. J., 2000, *Phys. Rev. D*, 62, 63511
- Klypin A., Kravtsov A. V., Valenzuela O., Prada F., 1999, *ApJ*, 522, 82
- Lacey C., Cole S., 1993, *MNRAS*, 262, 627
- Larson R. B., 1974, *MNRAS*, 169, 229
- Maller A. H., Dekel A., Somerville R., 2002, *MNRAS*, 329, 423
- Mathewson D. S., Ford V. L., Buchhorn M., 1992, *ApJS*, 81, 413
- Mestel L., 1963, *MNRAS*, 126, 553
- Mo H. J., Mao S., White S. D. M., 1998, *MNRAS*, 295, 319
- Monaco P., Theuns T., Taffoni G., 2002, *MNRAS*, submitted, astro-ph/0109323
- Moore B., Ghigna S., Governato F., Lake G., Quinn T., Stadel J., Tozzi P., 1999, *ApJL*, 524, L19
- Navarro J. F., Benz W., 1991, *ApJ*, 380, 320
- Navarro J. F., Frenk C. S., White S. D. M., 1995, *MNRAS*, 275, 56
- Navarro J. F., Frenk C. S., White S. D. M., 1996, *ApJ*, 462, 563 (NFW)
- Navarro J. F., Steinmetz M., 1997, *ApJ*, 478, 13
- Navarro J. F., Steinmetz M., 2000, *ApJ*, 538, 477
- Pagels H., Primack J. R., 1982, *Physical Review Letters*, 48, 223
- Peebles P. J. E., 1969, *ApJ*, 155, 393
- Porciani C., Dekel A., Hoffman Y., 2001, *MNRAS*, submitted, astro-ph/0105123
- Somerville R. S., Kolatt T. S., 1999, *MNRAS*, 305, 1
- Sommer-Larsen J., Dolgov A., 2001, *ApJ*, 551, 608
- Sommer-Larsen J., Gelato S., Vedel H., 1999, *ApJ*, 519, 501
- Springel V., Hernquist L., 2002, astro-ph/0111016
- Thacker R. J., Couchman H. M. P., 2000, *ApJ*, 545, 728
- Thacker R. J., Couchman H. M. P., 2001, *ApJL*, 555, L17
- Tytler D., Burles S., Lu L., Fan X., Wolfe A., Savage B. D., 1999, *AJ*, 117, 63
- van den Bosch F. C., 1998, *ApJ*, 507, 601
- van den Bosch F. C., Abel T., C. C. R. A., Hernquist L., White S. D. M., 2002, astro-ph/0201095
- van den Bosch F. C., Burkert A., Swaters R. A., 2001, *MNRAS*, 326, 1205 (BBS)
- Vitvitska M., Klypin A., Kravtsov A. V., Bullock J. S., Primack J. R., Wechsler R. H., 2001, *ApJ*, accepted, astro-ph/0105349
- Wechsler R. H., 2001, PhD thesis, Univ. California, Santa Cruz
- Weil M. L., Eke V. R., Efstathiou G., 1998, *MNRAS*, 300, 773
- Weinberg M. D., 1994, *AJ*, 108, 1398
- White S. D. M., Frenk C. S., 1991, *ApJ*, 379, 52
- White S. D. M., Rees M. J., 1978, *MNRAS*, 183, 341